

Sr, Nd, and Hf Isotope Compositions in Kimberlites and Carbonatites from South Africa: Constraints on Upper Mantle Metasomatism

Bizimis, M., NHMFL/FSU, Geology
 Salters, V.J.M., NHMFL/FSU, Geology

We report Sr, Nd, and Hf isotope, trace and rare earth element compositions in kimberlites and carbonatites from South Africa. Both rock types have very high LREE concentrations and steep REE patterns. The carbonatites show very strong depletions in Hf, Zr, and Ti relative to the adjacent REE. The kimberlite samples exhibit similar (although less prominent) depletions in Hf and Ti. We used the Hf isotopes to determine whether this depletion is a long-term feature of the mantle or a recent phenomenon. On a $\epsilon_{\text{Nd}}-\epsilon_{\text{Sr}}$ diagram (see Figure 1) these rocks plot within the Group 1 (G1) and Group 2 (G2) kimberlite fields.² On a $\epsilon_{\text{Nd}}-\epsilon_{\text{Hf}}$ diagram, G1 kimberlites plot below the OIB array having lower initial ϵ_{Hf} values ($\epsilon_{\text{Hf}} = -3.1$ to 2.7) for a given ϵ_{Nd} ($\epsilon_{\text{Nd}} = 0.3$ to 3.6). The G2 kimberlites plot at the extension of the array having unradiogenic compositions ($\epsilon_{\text{Nd}} = -9.2$ to -11.2 , $\epsilon_{\text{Hf}} = -7.8$ to -16). These compositions require that the G1 kimberlite source had time-averaged lower Lu/Hf and higher Sm/Nd ratios than a chondritic mantle.

Melting of a primitive or depleted upper mantle will increase both Sm/Nd and Lu/Hf ratios in the residue relative to a chondritic mantle. We propose that the low ϵ_{Hf} values (for a given ϵ_{Nd}) in the G1 kimberlite source are the result of metasomatism of a depleted mantle with a melt originating from a garnet peridotite. An initial depletion of the source is required to explain the positive ϵ_{Nd} values of the G1 kimberlites. The metasomatism by a garnet peridotite melt will reduce the Lu/Hf ratio in that source more

effectively than the Sm/Nd causing the Hf isotopic evolution to retard relative to Nd. Quantification of this model requires 1% initial depletion of a chondritic mantle at 2 Ga and metasomatism at 600 Ma to 800 Ma by a small degree melt from the same source. G2 isotopic compositions are model by the same process, but with the addition of a second component with the composition of the average crust. Given sufficient time after metasomatism (1.3 Ga) the G2 source will evolve to the observed negative ϵ_{Nd} and ϵ_{Hf} values. The presence of a crustal component in the G2 source is justified by the lower Ce/Pb and Nb/U ratios in G2 kimberlites relative to G1, and from earlier studies suggesting a G2 kimberlite origin from a long-stabilized subcontinental lithosphere.²

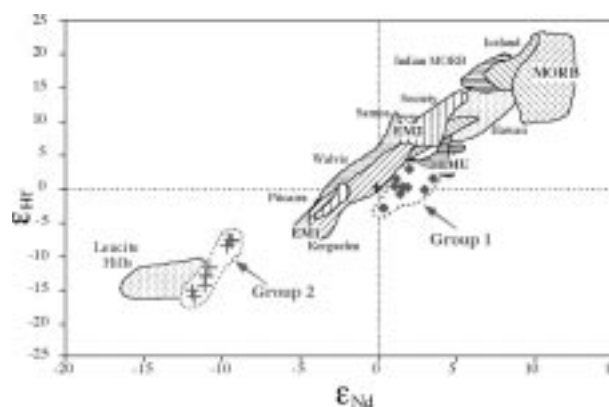


Figure 1. Hf-Nd isotope correlation diagram showing oceanic volcanoes and kimberlites.

The Hf depletion relative to Nd and Sm cannot be modeled by any melting and/or melt addition process in the mantle because of the similar compatibility of Sm and Hf in the upper mantle mineralogy. Furthermore, the concentrations in LREE and MREE in both G1 and G2 kimberlites are too high to be modeled without a very high (15%) melt addition in their source region. We suggest that a small (1%) addition of a carbonatite-type melt in the previously metasomatized kimberlite source can account for both the Hf depletion and the high LREE and MREE contents in the kimberlites. The lack of any correlation between the Hf depletion and the Hf isotopes, as well as the relative unradiogenic Hf isotope compositions

of the kimberlites suggests that this addition, and the subsequent Hf (and Ti) depletion of the kimberlite source has to be a recent feature or concomitant to the kimberlite genesis, and not a long lived characteristic of the mantle. Hf isotopes in carbonatites are currently under investigation but are expected to be similar to the kimberlites. The presence of at least two metasomatic events in the sublithospheric mantle has also been recently recognized in peridotite xenoliths from Tanzania.¹

References:

- ¹ Dawson, J.B., Proc. 7th Int. Kimberlite Conf., Cape Town, in press (1998).
- ² Smith, C.B., Nature, **304**, 51-54 (1983).

Vegetation Succession in a Coastal Wetland in Northwest Florida: Evidence from Stable Carbon Isotopes

Choi, Y., NHMFL/FSU, Geology

Wang, Y., NHMFL/FSU, Geology

Measurements of stable C isotopic ratios, as well as C, N, and P inventories in soils and plants, were made along a transect stretching from high marsh through middle marsh to low marsh in a coastal wetland in northwest Florida. The wetland is dominated by *Juncus roemerianus*, which is a C₃ plant and has an average $\delta^{13}\text{C}$ of -27‰ . Lesser amounts of *Spartina alterniflora*, which is a C₄ plant and has an average $\delta^{13}\text{C}$ value of -13‰ , and some other species, are also present in the area. The $\delta^{13}\text{C}$ values of soil organic matter from low and middle marshes range from -24 to -27‰ , which are consistent with the current plant community. However, the $\delta^{13}\text{C}$ values of soil organic matter from high marsh show significant variations, from -23‰ in the surface soil to -17‰ at depth (Figure 1). This large C isotopic variation within soil profiles indicates a shift in local vegetation, from a C₄ (e.g., *Spartina alterniflora*) dominated community to the current C₃ plant (*Juncus roemerianus*) dominated community as coastal wetland evolves from high marsh to middle marsh

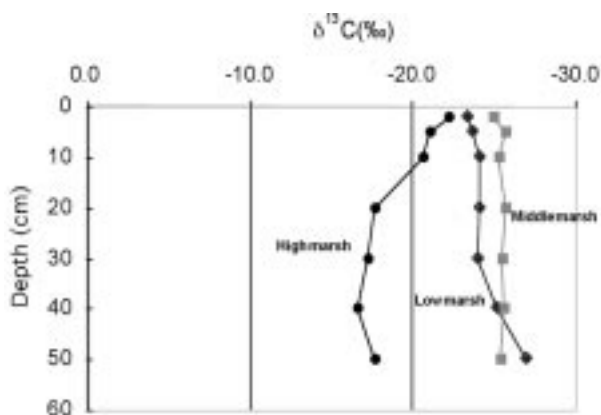


Figure 1: Stable carbon isotopic composition of soil organic matter in a coastal wetland in Northwest FL (St. Marks, Wakulla Co.).

and low marsh. Soil organic carbon inventory was about 31 kg/m² in low marsh, 19 kg/m² in middle marsh, and 18 kg/m² in high marsh. The much higher C storage in low marsh than in high marsh indicates that carbon sequestration increase significantly as coastal wetland evolves from high marsh (initial stage) to low marsh (steady state). N and P inventories are also higher in low marsh than in high marsh, and seem to correlate directly with above-ground productivity in the marshes. This has important implications to the global C cycle. As sea level rises due to global warming, coastal wetlands are expected to expand landward, which would provide a significant sink for atmospheric carbon dioxide.

Characterization of Organic Nitrogen Compounds in Aquatic Fulvic Acid Mixtures by High Resolution Multistage (MSⁿ) FT-ICR Mass

Cooper, W., FSU, Chemistry

Llewelyn, J., FSU, Chemistry

Fiebre, A., FSU, Chemistry

Marshall, A., NHMFL/FSU, Chemistry

A fundamental paradigm of modern aquatic biogeochemistry is that biomass production in most surface waters (marine, estuarine, and terrestrial) is either nitrogen or phosphorous limited. While the

relationship between inorganic forms of these important nutrients (e.g. NH_4^+ , NO_3^- , NO_2^- ; H_2PO_4^- , and HPO_4^{2-}) and primary productivity is fairly well understood, dissolved organic nitrogen (DON) and dissolved organic phosphorous (DOP) have been conspicuously absent from most nutrient flux models. This is in spite of the fact that DON constitutes nearly 100% of available nitrogen in oligotrophic systems, and DOP can represent more than 50% of total phosphorous in certain wetlands.

The current lack of understanding about the role of DON and DOP in primary and secondary aquatic production is due in great part to a lack of analytical methods capable of providing specific molecular information (i.e. molecular weights, chemical formulae) about individual components that comprise the organic nutrient pool in natural waters. In a previous report, we demonstrated that high resolution Fourier transform ion cyclotron resonance mass spectrometry at 9.4 T could provide reasonable estimates of the chemical formulae of individual components in aquatic fulvic acid mixtures.¹ Additional experiments carried out this year were designed to determine exact molecular formulae of organic nitrogen compounds in aquatic fulvic acid mixtures. These experiments involved Stored Waveform Inverse Fourier Transform (SWIFT) isolation of parent ions in a very narrow m/z window, IR Multiphoton Dissociation (IR-MPD), and high resolution FT-ICR MS of the daughter ions produced.

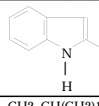
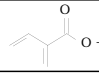
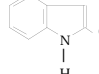
High resolution single stage FT-ICR MS ($m/\Delta m > 500,000$) was used to identify the ten most prominent peaks in the aquatic fulvic acid mixture spectrum that contained nitrogen. These ten peaks were then subjected to the multistage (MS) scheme. The results

Table 1. Mass and proposed molecular formulae of ten ions selected from the fulvic acid spectrum the corresponding fragment ions produced by IR-MPD.

| Parent ion mass (m/z) | Molecular formula* | Fragment ion mass (m/z) | Molecular formula* | Fragment lost |
|---------------------------|--------------------|-----------------------------|--------------------|---------------|
| 300.434 | C18H40N2O | 240.503 | C16H34N | C2H6NO |
| 315.327 | C18H41N3O | 255.392 | C17H37N | CH4N2O |
| 374.45 | C18H46N8 | 357.441 | C18H43N7 | NH3 |
| 375.279 | C23H37NO3 | 315.326 | C21H33NO | C2H4O2 |
| 379.356 | C23H45N3O | 319.401 | C21H39N2 | C2H6NO |
| 383.454 | C23H47N2O2 | 307.427 | C22H43 | CH4N2O2 |
| 398.292 | C23H36N5O1 | 338.332 | C21H30N4 | C2H6NO |
| 427.48 | C25H57N5 | 367.512 | C23H49N3 | C2H8N2 |
| | | 293.503 | C20H39N | unknown |
| 439.361 | C17H45N9O4 | 333.417 | C14H39N9 | C3H6O4 |
| 455.328 | C28H43N2O3 | 395.351 | C28H43O | N2O2 or 2(NO) |

of these experiments are summarized in Table 1, which contains the proposed molecular formulae of the ten ions in the aquatic fulvic acid spectrum chosen for MSⁿ analysis, along with the formulae of the most prominent fragment ions produced from each parent ion, and the fragments that were lost in the IR-MPD step.

Table 2. Masses and proposed structures of ten ions selected from the HPLC fractionation of standard fulvic acid mixtures, along with the corresponding fragment structures.

| Molecular Weight | Proposed Structure |
|------------------|---|
| 300.434 | $\text{CH}_3(\text{CH}_2)_{12}(\text{CH}-\text{NH}_2)_2\text{O}-(\text{CH}_2)_2\text{CH}_3$ |
| 315.327 | $\text{HN}-\text{CHCH}_2\text{NH}_2(\text{CH}_2)_8(\text{CH}-\text{NH}_2)_3\text{O}-(\text{CH}_2)_2\text{CH}_3$ |
| 374.45 | $\text{CH}_3(\text{CH}_2)_{10}(\text{CH}-\text{NH}_2)_7\text{NH}_2$ |
| 375.279 | $\text{CH}_3(\text{CH}_2)_2\text{O}-(\text{CH}-\text{NH}_2)_2(\text{CH}_2)_8(\text{CH}-\text{NH}_2)_3\text{O}-(\text{CH}_2)_2\text{CH}_3$ |
| 379.356 | $\text{CH}_2=\text{CH}(\text{CH}_2)_{17}\text{CH}=\text{CHCH}-\text{NH}_2\text{O}-(\text{CH}_2)_2\text{CH}_3$ |
| 383.454 | $\text{CH}_2=\text{CH}(\text{CH}_2)_{18}\text{CH}-\text{NH}_2\text{O}-\text{CH}-\text{NH}_2\text{CH}_2\text{NH}_2$ |
| 398.292 |  |
| 427.48 | $\text{CH}_2=\text{CH}(\text{CH}_2)_{14}(\text{CH}-\text{NH}_2)_5\text{O}-(\text{CH}_2)_2\text{CH}_3$ |
| 439.361 |  |
| 455.328 |  |

Proposed molecular structures of the ten chosen ions, as well as structures for the daughter-ion fragments, are summarized in Table 2. These structures are suggested based on our high resolution MS-MS measurements, as well as MS data obtained by Schulten² using pyrolysis techniques.

These structures, if supported by additional high-resolution MS/MS experiments, would provide the first direct evidence that nitrogen in surface waters can be stored for long periods (> 100 years) in large, high molecular weight organics such as fulvic acids, and brings into question the bioavailability of organic nitrogen. Parallel high resolution FT-ICR MS studies of organic phosphorous are also underway, in conjunction with bioavailability assays being carried out in the FSU Department of Oceanography.

This work was supported by the St. Johns River (FL) Water Management District; the South Florida Water Management District; Florida State University; and the N.S.F. High-Field FT-ICR Mass Spectrometry Facility (CHE-94-13008) at the National High Magnetic Field Laboratory.

References:

- 1 Fiebre, A., *et al.*, Energy & Fuels, **11**, 554-560 (1997).
- 2 Schulten, H.R., *et al.*, Humic Substances in the Global Environment and Implications on Human Health 43-56 (1994).

Pb Isotopes in Tree Rings: Chronology of Pollution in Bayou Trepagnier, Louisiana

Marcantonio, F., Tulane Univ., Geology and Molecular Biology

Flowers, G., Tulane Univ., Geology and Molecular Biology

Thien, L., Tulane Univ., Geology and Molecular Biology

Ellgaard, E., Tulane Univ., Geology and Molecular Biology

We have measured the Pb isotopic composition of tree rings from seven trees in both highly contaminated and relatively non-contaminated regions of Bayou Trepagnier, a bayou in southern Louisiana that has had oil refinery effluent discharged into it over the past 70 years. To our knowledge, this is the first time that Pb isotope tree ring records have been used to assess the sources and extent of heavy-metal contamination of the environment through time. When tree ring $^{206}\text{Pb}/^{208}\text{Pb}$ and $^{206}\text{Pb}/^{207}\text{Pb}$ isotope ratios are plotted against one another, a straight line is defined by four of the most contaminated trees. This linear correlation suggests mixing between two sources of Pb. One of the sources is derived from the highly polluted dredge spoils on the banks of the bayou, and the other from the natural environment. The nature of the contaminant Pb is unique in that it is, isotopically, relatively homogenous, and extremely radiogenic, similar to ores of the Mississippi Valley (i.e., $^{206}\text{Pb}/^{207}\text{Pb} = 1.28$). This singular pollutant isotope signature has enabled us to determine the extent of Pb contamination in each cypress wood sample. The isotope results indicate that Pb uptake by the tree is dominated by local-scale root processes and is, therefore, hydrologically and chemically controlled. In addition, we propose that the mobility and bioavailability of Pb in the environment depends upon its chemical speciation.

Reference:

- 1 Environmental Science and Technology, **32**, 2371-2376 (1998).

High Precision Measurement of Mercury Isotopes by Secondary Ionization Mass Spectrometry: Potential as Environmental Tracers

Mitchell, S., NHMFL/FSU, Geology

Odom, A.L., NHMFL/FSU, Geology

Natural variations that occur in the isotopic composition of chemical elements in the Earth result from nuclear processes such as radioactive decay and cosmic-ray spallation effects, as well as the consequences of atomic and molecular energy/mass partitioning effects. Mass fractionation of isotopes of a number of elements has produced variations in isotope ratios that have been used as tracers of geochemical and geologic processes. Until this study, the existence of measurable, natural, isotopic variations has not been demonstrated unequivocally in elements of atomic numbers greater than 34.

Consideration of the chemical and physiochemical behavior of mercury led us to suspect that of all the heavier elements, mercury seemed to be the most likely to possess isotopic variations large enough to measure, provided such measurements could be made with a 10-fold improvement of precision over previously reported attempts. The impetus for this effort are the questions regarding the origin of the high level of mercury that has begun to accumulate (during this century) in aquatic animals, on what appears to be hemispherical, if not global, scale. There is a chance that, if mercury isotopes are fractionated during geochemical and biogeochemical reactions, isotope ratios could provide natural tracers of sources and pathways of environmental mercury.

Mercury is obtained from its ore mineral Cinnabar (HgS , trigonal), by roasting in air, and condensation followed by distillation. Samples of cinnabar from

several different mining districts have been selected in an attempt to determine the isotopic composition of mercury, prior to industrial processing and environmental cycling. Mercury isotope ratios were measured with the NHMFL modified ISOLAB-54, magnetic sector, secondary-ionization, and mass-spectrometer. This instrument is fitted with a duoplasmatron primary ion source, moveable Faraday cups for simultaneous measurement of ion currents, and a Daly detector.

Screens were set for analyses as minimum strengths of ion currents and internal precision of the run. Each analysis consisted of 70 to 100 measurements of isotope ratios. The graph is a plot of isotope ratio pairs, $^{200}\text{Hg}/^{202}\text{Hg}$ versus $^{198}\text{Hg}/^{204}\text{Hg}$ as measured in the cinnabar samples. Also plotted are ratios measured in two industrially processed samples of mercury (IND-1 and IND-2). The solid line drawn is a best fit line to the cinnabar data. The cross lines drawn on samples 2, 3, and 6a represent two standard deviations of the means, and is a measure of the internal precision of the run. For the remaining samples this uncertainty is either equivalent to or less than that of 2, 3, and 6a. The dashed line is a theoretical, mass-fractionation curve.

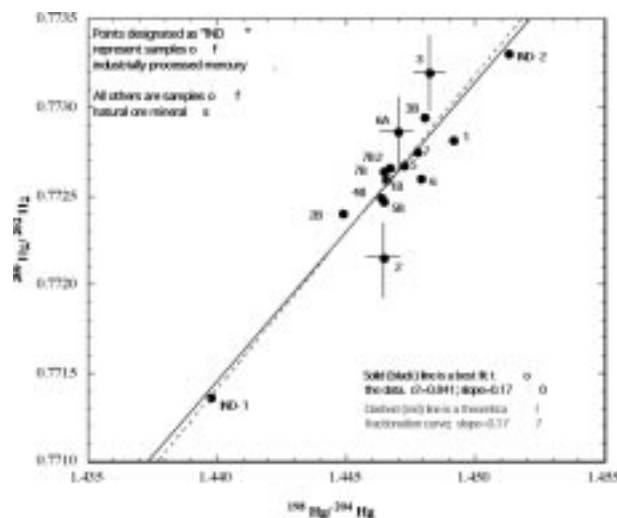


Figure 1. Plot of $^{200}\text{Hg}/^{202}\text{Hg}$ vs. $^{198}\text{Hg}/^{204}\text{Hg}$ for cinnabar samples.

That the values measured for the industrially processed mercury lie along a fractionation curve that is indistinguishable from the best fit line for the cinnabar samples strongly suggest that the range in isotope ratios measured (about 7 permil) is due to mass fractionation. The data seems to indicate isotopic differences between

the cinnabar samples. Such differences might be the result of the diffusive processes involved in the formation of cinnabar in the cooling, epithermal haloes of igneous intrusions. The isotopic composition of the industrially processed mercury IND-1 is clearly heavier than the unprocessed mercury ores, while IND-2 appears to be somewhat lighter.

Future efforts will center on developing techniques for high precision isotopic analyses on environmental mercury at low concentration levels.

Phosphorous Analysis in Natural Waters by Inductive Coupled Plasma Mass Spectrometry

Salters, V.J.M., NHMFL/FSU, Geology
Bennett, L., NHMFL/FSU, Geology

Phosphorous is the limiting nutrient in the aquatic ecosystem of the Everglades. Presently, the Everglades ecosystem is being destroyed by the runoff from agricultural, as well as urban areas, where waters are high in phosphorous. There are several research efforts underway into the best treatment that lowers the phosphorous content of the waters entering the Everglades. Development and testing of these techniques requires development of a new analytical technique that allows analysis of phosphorous at lower concentration levels. We have developed such a technique. This new analytical technique is a crucial tool needed for the determination of the speciation and bioavailability of phosphorous. Phosphorous concentration in the pristine Everglades is below the detection limit of the conventional techniques. In addition, phosphorous speciation requires the ability to measure phosphorous at the sub ppb level. With this new technique we are able to address the cycling and the speciation of phosphorous in the Everglades.

Phosphorous is measured on a high resolution inductively coupled plasma mass spectrometer at mass resolution of 3000. This mass resolution allows separation of the isobaric $^{15}\text{N}^{16}\text{O}$ interference on ^{31}P . Fresh water samples are acidified with nitric acid (to 1%) before analysis.

The detection limit (0.3 ppb P for ICP-MS; calculated as three times the standard deviation of the blank measurement) for ICP-MS is lower than the detection limit for the conventional calorimetric method (detection limit is between 3 and 5 ppb P), and thus, for the low level measurement the ICP-MS is deemed to provide, as expected, a better analysis. We have validated the technique by replicate analysis by conventional methods, and through partaking in an intercomparison between laboratories in Florida. Figure 1 shows the excellent agreement between the ICP-MS technique and conventional technique at phosphorous levels above 10 ppb. Especially at levels below 10 ppb P the blank corrections for the calorimetric method are large, and the ICP-MS method is deemed to be the better one.

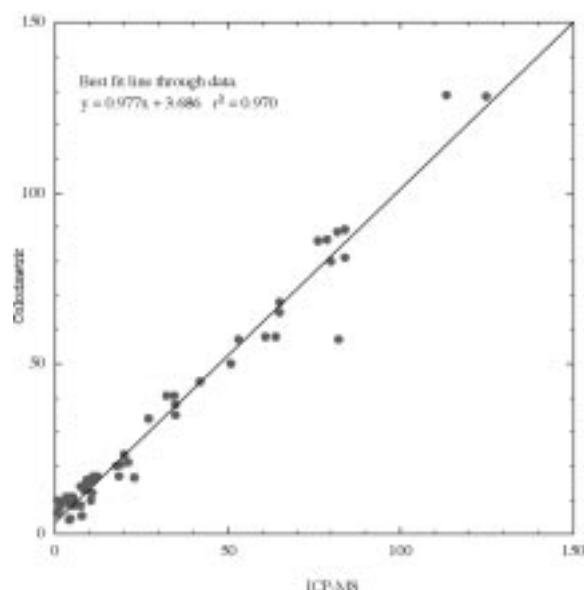


Figure 1. Comparison between ICP-MS and colorimetric phosphorous analyses.

Trace Element Partitioning Constraints on Melting Beneath Mid-Ocean Ridges

Salters, V.J.M., NHMFL/FSU, Geology
Longhi, J., Columbia Univ., Lamont-Doherty Earth Observatory

In our effort to characterize the trace element partitioning behavior during melting beneath

mid-ocean ridges, we have expanded the pressure and temperature conditions of our experiments to both higher (up to 3.2 GPa) and lower pressures (down to 1.5 GPa). Our experiments are the first experiments that closely mimic the pressure-temperature-composition conditions under which primary melts are formed beneath mid-ocean ridges. In determining the phase compositions of the anhydrous lherzolite, we found that the composition of the clinopyroxene on the anhydrous solidus changes from high-Ca to low-Ca with increasing pressure.

Figure 1 compiles the partitioning data we have obtained up till recently. The range in partition coefficients is caused by the different conditions under which the individual phases were grown. For clinopyroxene it was found that next to pressure and temperature, the Ca-content of the clinopyroxene has a large influence on the partition coefficients. For garnet, next to P and T, the Ca-content in the garnet and the Mg-Fe ratio of the melt influences the partitioning behavior.

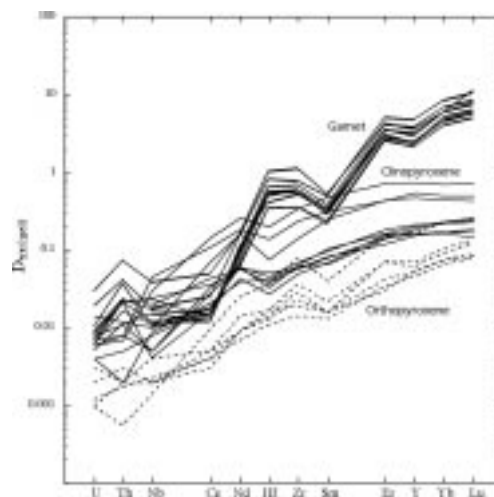


Figure 1. Partition coefficients for garnet/melt (heavy lines), clinopyroxene/melt (thin lines) and orthopyroxene/melt (dashed lines).

Our D_U and D_{Th} for garnet, which are the most appropriate yet for melting of four phase lherzolite, predict larger fractionations of U and Th for comparable conditions than previous sets of coefficients. These larger fractionations are mostly due to the higher values of the D_s for garnet, which create a greater leverage of garnet on the bulk

partition coefficients. Model calculations using the new partition coefficients are shown in Figure 2.

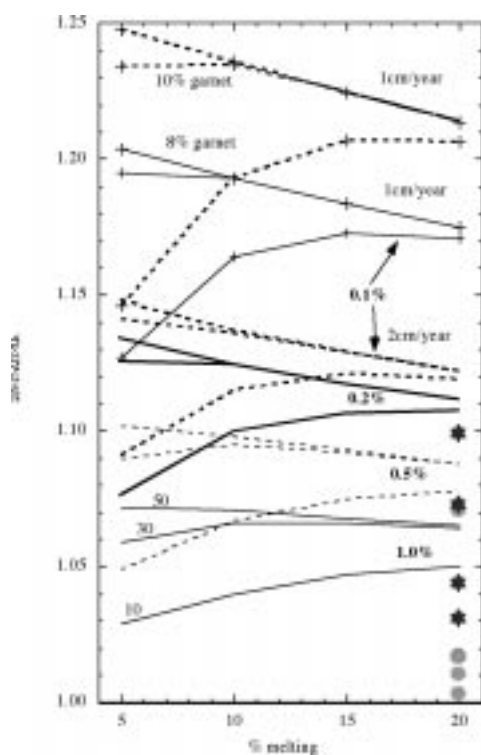


Figure 2. ^{230}Th excesses vs. degree of melting. Dependence of ^{230}Th excesses on a number of parameters is shown. Each line represents calculations of melting curves for a fixed set of parameters. Calculations are presented in groups of 3 melting curves (identical line type) representing varying amounts of melting in the garnet stability field (10 %, 30%, and 50%). The three melting curves are grouped according to porosity. At more than 15% melting there is no overlap in ^{230}Th excesses between the groups. Melting curves without symbols represent mantle matrix ascent rates of 2 cm/yr, and melt ascent rates of 400 cm/yr at varying porosities. Except for bold hatched curves with symbols all other curves are with 8 modal % garnet in the initial source. Amounts of melting in the garnet stability field are presented as amounts of melting of the on-axis melting column. The data is compared with Spiegelman and Elliott (1993), and taken from their Figures 8a and b. The circles represent their model with parameters (as similar as possible) for disequilibrium transport and using D 's for garnet;¹ different circles are for different porosities (1%, 0.5%, and 0.1%); smallest excess ^{230}Th is created with the highest porosity. The stars are the same models, but "equilibrium" melt transport.

Figure 2 shows that the new partition coefficients are able to achieve significant ^{230}Th excesses at higher porosities than previously possible, and that average ^{230}Th excesses of 10% in mid-ocean ridge basalts can be achieved with porosities from 0.2% to 1%. These porosities are in agreement with recent results of seismic tomography beneath the East Pacific Rise, which indicate the presence of up to a 1% melt.³

References:

- 1 Beattie, P., *Nature*, **363**, 63-65 (1993).
- 2 Spiegelman, M., *et al.*, *Earth Plan. Sci. Lett.*, **118**, 1-20 (1993).
- 3 Toomey, D.R., *et al.*, *Trans AGU*, **78**, 705 (1997).

Partial Melting of the Earth's Mantle Beneath Theistareykir, Northern Iceland

Stracke, A., NHMFL/FSU, Geology

Zindler, A., NHMFL/FSU, Geology

Blichert-Toft, J., Ecole Normale et Supérieure de Lyon, France

Albarède, F., Ecole Normale et Supérieure de Lyon, France

As part of our investigation of Icelandic volcanism, we use isotopic ratios of elements such as Hf, Nd, and Sr, as petrogenetic tracers to study melting processes, and the composition and chemical evolution of the Earth's mantle beneath Iceland.

Hf, Nd, and Sr isotope ratios reflect the chemical composition and time-integrated chemical evolution of the Earth's mantle. Excellent correlations between Hf, Nd, and Sr isotope ratios indicate mixing of at least two distinct source components: one is similar to an upper mantle source, which evolved with a time-integrated depletion in incompatible trace elements, and the other evolved with a relative enrichment in incompatible trace elements.

Major and trace element concentrations and ratios (including MgO , FeO , Na_2O , $\text{CaO}/\text{Al}_2\text{O}_3$, $\text{K}_2\text{O}/$

TiO₂, La/Sm, etc) are also correlated with Hf, Nd, and Sr isotope ratios (e.g., Figure 1). In contrast to the isotope ratios, these parameters are expected to undergo significant modification during fractional crystallization of the melts in upper crustal magma chambers, and hence any pre-existing correlation between major element concentrations and isotope ratios is usually destroyed by fractional crystallization processes. These correlations can, therefore, only be explained if the major element compositions of the primary melts are not significantly changed during fractional crystallization, or if melts from different sources have systematically different fractionation histories, which is unlikely. Since the above mentioned parameters are also an indication of the degree and pressure of melting in the Earth's mantle, the correlation of these parameters with the isotope ratios suggest that there is a relationship between the melting process and the chemical composition of the melted mantle (as reflected by the isotopic composition of the melts).

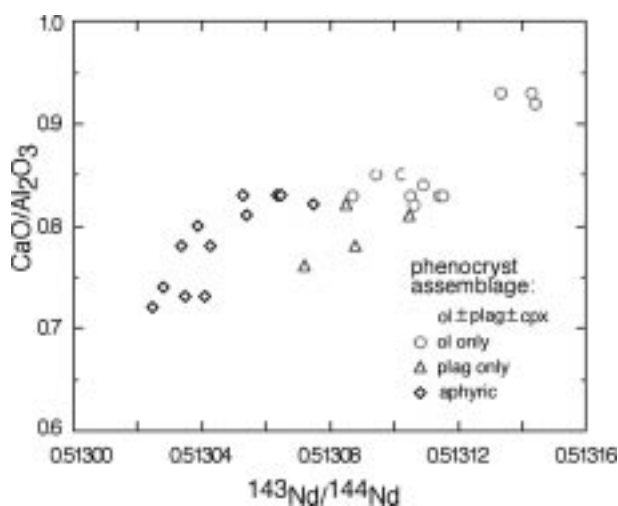


Figure 1. The CaO/Al₂O₃ and ¹⁴³Nd/¹⁴⁴Nd ratios in the Theistareykir basalts are positively correlated. The CaO/Al₂O₃ ratio increase with increasing degree of melting, therefore, the highest degree melts are derived from the most depleted sources (highest ¹⁴³Nd/¹⁴⁴Nd).

This interpretation is further substantiated by comparing the range of compositions of the Theistareykir basalts with primary melt compositions (i.e., melts that are not modified by fractional crystallization) as calculated.¹ The

Theistareykir basalts follow a trend of primary melt compositions,² suggesting that the variable major element compositions are mainly a result of the melting process. It can be inferred from Figure 2 that different degree melts are also derived from chemically different source components.

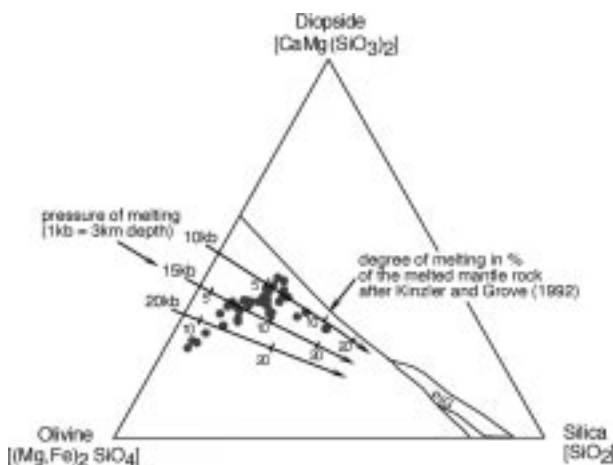


Figure 2. Comparison of the Theistareykir melts with primary melt compositions;¹ showing that the Theistareykir basalts follow a melting.²

There are a variety of ways to explain the isotopic heterogeneity of the source, including the incorporation of an enriched mafic component (possibly ancient subducted basalt) within ambient depleted peridotite, the entrainment of ambient depleted mantle in an isotopically enriched mantle plume, or even the redistribution of a small melt fraction within an essentially homogeneous peridotite at some time in the distant past. No matter which model is preferred, a difference in solidus temperature of the two isotopically distinct components has to be invoked in order to account for the observed relationship between Hf, Nd, and Sr isotope ratios and major and trace element concentrations and ratios.

References:

- 1 Kinzler, R.J., *et al.*, J. Geophys. Res., **97**, 6885-6906 (1992).
- 2 Kinzler, R.J., *et al.*, J. Geophys. Res., **97**, 6907-6926 (1992).

Carbon Isotope Evidence for Environmental Change in Nihewan Basin, China

Wang, Y., NHMFL/FSU, Geology

Dong, J., Chinese Academy of Science, Institute of Vertebrate Paleontology and Paleoanthropology

Amundson, R., Univ. of California-Berkeley, Environmental Science, Policy and Management

Nihewan Basin, in northeast China, is well known for its abundant Paleolithic stone tools, and well-exposed Quaternary sedimentary sequences. The deposits in the basin are primarily composed of lacustrine and fluvial sediments, spanning continuously a time period from Pliocene to Holocene. The results of isotopic analysis of fossil tooth enamel from several archaeological sites of Pleistocene age in Nihewan Basin show significant changes in paleoenvironment (Figure 1).

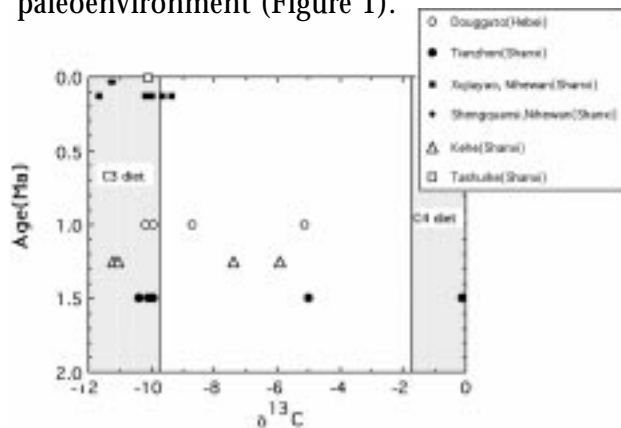


Figure 1. Carbon isotopic composition of tooth enamel from northern China. It shows that C4 grasses were a significant component of herbivores' diet during early and middle Pleistocene, and became insignificant in late Pleistocene. This dietary change might be due to a change in climate and local ecology.

The $\delta^{13}\text{C}$ values of early Pleistocene-age samples range from -10.4‰ to -0.1‰, indicating that herbivores had a variety of diet, ranging from pure C3 to pure C4 plants. This suggests that C4 grasses were a significant component of the local ecosystem in the early Pleistocene.

The $\delta^{13}\text{C}$ values of middle Pleistocene samples are -11.3‰ to -5.1‰, indicating that herbivores' diet was composed of pure C3 to mixed C3/C4 plants, and C4 grasses were still an important component of the local flora in the middle Pleistocene.

On the other hand, late Pleistocene-age samples have $\delta^{13}\text{C}$ values of -9‰ to -11.7‰, indicating that herbivores were predominantly eating C3 vegetation, and the local ecosystem was dominated by C3 plants (e.g. trees and shrubs) in the late Pleistocene.

This habitat change has important implications for understanding the effects of environmental change on the evolution and cultural development of *Homo erectus* in eastern Asia.

EPR Investigations of High-Level Dosimetry in Quartz: Radiation Sensitivities

Xie, J.P., NHMFL/FSU, Geology

Odom, A.L., NHMFL/FSU, Geology

Investigations continued this year into the high level dosimetric properties of quartz. Particular consideration was given to $[\text{GeO}_4/\text{Li}^+]$, E_1' , E_4' , and other oxygen vacancy-related centers that are typically observed in EPR powder spectra as large, broad (RT) resonance lines consisting of (from lower to higher magnetic field), a non-bridging oxygen hole center (NBOHC), a middle peak MP (model yet developed), and a proxy radical center. These EPR centers result from the trapping of radiation-produced, band-gap charges at point defects (Ge impurities and Schottky-Frenkel pairs). The findings reported here are the results of γ radiation experiments up to the gigrad level. Quartz samples used in this study were separated from volcanic and hypabyssal intrusive rocks of known age (ranging from 7×10^5 to 1.4×10^9 years), and measured radioactivity.

With increasing doses of γ radiation, growth in the intensity of the resonance peaks increased in two stages: 1) exponential growth at lower dose levels (up to 10^7 to 10^8 rads for E_1' centers) that reflects the trapping of charges (holes in the case of E_1' centers) by existing precursors (oxygen vacancies in the case of E_1'); followed by 2) slower linear growth that is dominated by the radiolytic production of new vacancies.

EPR signal intensities I of the E_1' , NBOHC, and MP can be well described by the equation:

$$I = I_n + (I_m - I_n)(1 - \exp^{-c\gamma}) + \kappa\gamma$$

where I_n is the intensity of the native signal in quartz (i.e. where the dose absorbed is only from the ambient radiation in the host rocks of the quartz), I_m is the maximum EPR intensity achieved during exponential growth, c is the radiation sensitivity constant, during exponential, κ is the radiation sensitivity constant for the radiolytic production of new traps, and γ is the radiation dose.

The values of c and k were determined for each of a suite of quartz samples. Because sensitivities depend on the nature and abundance of competing electron and hole traps, their values are unique for each specimen of quartz. For the E_1' center, the values of c ranged from 1.57×10^{-7} to 6.23×10^{-8} . The sensitivity, κ , increases linearly with TND (total natural dose); TND is determined from the age of the host rock and its radioactivity. This study is part of an ongoing effort to develop a useful quartz geochronometer.

A Comparison of Modern Mass Spectrometric Methods for Th Isotope Ratio Measurement

Zindler, A., NHMFL/FSU, Geology

Reid, M., Univ. of California-Los Angeles, Earth and Space Science and IGPP, W.M. Keck Foundation Center for Isotope Geochemistry

Albarede, F., Laboratoire des Sciences de la Terre

Blichert-Toft, J., Laboratoire des Sciences de la Terre

Since 1986, when the first measurements of Th isotope ratios in corals were published,³ numerous advances have been made in the measurement of Th isotope ratios by mass spectrometry. As a result, new avenues for research using the U-Th disequilibrium system have been successfully exploited, including high-precision re-calibration of the Pleistocene sea-level curve,¹ the investigation of magma dynamics, and the timing of eruptions in continental and oceanic settings,^{4,6} and the use of U-Th disequilibrium as a "tracer" for processes that affect mantle sources prior to and during magnetism.² Despite these advances, made possible by the smaller sample requirements and higher precision of mass spectrometry over the older alpha spectroscopy method, the dating of volcanic rocks, and authigenic or biogenic sediments (other than corals), over the past 400 to 500 kyr., have yet to be established as routine methods. Because of the potential importance of these dating techniques to the fields of paleoclimatology and volcanology, isotope geochemists have continued to focus on the development of newer and better techniques for the measurement of Th isotope ratios in even smaller samples.

The measurement of Th isotope ratios by TIMS has generally yielded ionization-plus-transmission efficiencies (hereafter, simply "efficiencies") of about 5×10^{-5} to 10^{-4} in volcanic rocks, although an order of magnitude improvement can be achieved for corals, because of their relatively low

$^{232}\text{Th}/^{230}\text{Th}$ ratios, and the resulting ability to analyze far smaller samples of total Th than is possible with volcanic rocks (thermal ionization efficiency increases as the total amount of Th in a sample decreases³). While the TIMS method permits the analysis of most volcanic rocks, it is best suited to those that are relatively high in Th, because low-Th rocks, such as MORBs, still typically require the preparation of more than one gram of uncontaminated material, which is a non-trivial task at best. In contrast, the thermal technique is perfectly suited to coral analysis, due to high U concentrations, and the ready availability of relatively large amounts of sample material.

The measurement of Th isotope ratios by SIMS, first achieved using the Lamont Isolab 54 mass spectrometer, afforded a routine increase in efficiency of about a factor of ten over TIMS (~0.1%), making the analysis of MORBs and medium to high Th content phenocrysts from volcanic rocks far easier.² Improvements to the SIMS Th technique using the Isolab, now situated at the NHMFL, show the promise of efficiencies in the range of 2% to 5% (though, to date, this has been demonstrated only for standards), a level at which low Th phenocrysts, perhaps even in MORBs, and low-U marine carbonates, may become amenable to analysis.

The new Cameca 1270 Ion Microprobe at UCLA has been shown to permit in situ Th isotopic analysis of zircons and allanites, leading the way to entirely new applications in the study of magma system evolution and dynamics.⁷ Furthermore, experiments with chemically separated Th, loaded using the technique developed for the Isolab, show that the 1270 and the Isolab yield similar ionization efficiencies. The addition of multi-collector capability to this instrument in the near future will undoubtedly lead to further improvement in its Th analysis capability.

Perhaps the most exciting of the new techniques for Th isotope ratio measurement has seemed to be the multi-collector ICP-MS.⁵ Experiments with the Plasma 54 in Lyon have demonstrated the

capability for ionization efficiencies in the 0.1% to 0.5% range, similar to the SIMS results. However, the ease of sample preparation for this type of analysis, especially compared to that required for SIMS, makes it a very attractive alternative for many applications. Contamination of the tubing in the sample inlet system is a concern, but can be overcome by sustained washing between samples, or the addition of a carrier element to the Th sample solution.

A limitation for all of these techniques has been the accurate and precise intercalibration of the ion-counting and faraday detection systems, due to the high dynamic ratios characteristic of most Th samples. While precisions in the range of 0.1% 2σ for $^{230}\text{Th}/^{232}\text{Th}$ ratios are theoretically possible, this level of precision has never been obtained. Though in part due to detector intercalibration uncertainties, the problem has received less attention than it might have, due to the fact that, for most applications, where increased precision would be desirable, sample size limitations more-or-less precluded attainment of precisions better than 0.5% to 1.0%. As we look now to the ability to analyze much smaller samples of Th, in part due, perhaps, to the ability to process much larger total samples for ICP-MS analysis, detector intercalibration will increasingly become a more important issue. We have developed a technique, similar to that discussed by Luo,⁵ which involves the addition of a specially prepared U standard to Th samples being readied for SIMS or ICP-MS analysis. The standard, which is similar to NBL U500, but with $^{234}\text{U}/^{238}\text{U}$ ratio of about 5×10^{-5} , can be used to obtain an interdetector calibration at the 0.1% level or better, without resorting to peak-switching intercalibration at relatively high intensities, or assuming a linear response for the ion-counting detection system over many orders of magnitude in count rate.

Experiments with all systems are currently underway, and new results will be presented.

References:

- 1 Bard, E., *et al.*, *Nature*, **345**, 405-409 (1990).
- 2 Bourdon, B., *et al.*, *Nature*, **384**, 231-235 (1996).

- ³ Edwards, R.L., *et al.*, *Earth Planet Sci. Lett.*, **81**, 175-192 (1986-87).
- ⁴ Goldstein, S.J., *et al.*, *Earth Planet Sci. Lett.*, **96**, 134-146 (1989).
- ⁵ Luo, X., *et al.*, *EOS*, **78**, 46, 787 (1987).
- ⁶ Reid, M.R., *Earth Planet Sci. Lett.*, **131**, 239-254 (1995).
- ⁷ Reid, M.R., *et al.*, *Earth Planet Sci. Lett.*, **150**, 27-39 (1997).

Age and Isolation of Mantle Components and Reservoirs: A Question of Model Dependence

Zindler, A., NHMFL/FSU, Geology

The survival of chemically distinct materials in the mantle over significant periods of Earth history is beyond debate. In using this information to help constrain the structure, evolution and dynamics of the mantle, the important questions are how long such materials can be isolated, in what volumes, and where. While the most vivid descriptions of mantle materials arguably come from geochemical studies, geochemistry can only directly address the first of these questions, and then, only in a model-dependent fashion. These models that investigators in all fields of mantle study rely on contain elements that derive from every discipline, elements that have been refined and developed over the past twenty years. Why is it, then, that with the major advances that have occurred, many of the fundamental questions that were posed twenty years ago, remain unanswered today, for example, those relating to the preservation and destruction of chemically distinct materials?

Perhaps the answer is simply that the problems are so immense that more time, more money, and more effort is required. I am inclined to believe, however, that our efforts are hindered by the difficulty in organizing the myriad of available constraints in terms of their importance, their assuredness, and their relationships to one

another—and possibly by our tendency to give more credence to those we better understand, those we do not understand at all and must take on faith, or those we play some personal role in delineating. With all the fun, the most important step is often forgotten, to critically evaluate the new constraint, and place it clearly and objectively within the existing framework. Geochemists, for example, have suggested that noble gas budgets and isotope ratios require the long-term isolation of large scale domains within the mantle. While these constraints are important, they have been overstated. The arguments imply that noble gases are special. However, below the relatively shallow depths where melts are present, and where a gas phase can separate from a liquid magma (of paramount importance during accretion), noble gases are not so different from other elements. Studies of their partitioning suggest that, in terms of solid-liquid equilibria, they are less incompatible than elements like U and Th. Therefore, identification of a mantle segment inferred to contain Ar or He, which requires isolation for the past 2 Ga. or longer, is no more (or less) compelling an argument for isolation of the lower mantle than one built on the basis of Nd, Sr, or Pb.

He that contains relatively large amounts of ^3He is conventionally considered to be “primitive”. In this context, “primitive” means least affected by radiogenic accumulation since accretion. Applying this same criteria, the most “primitive” Sr and Pb is found in MORBs, while the most “primitive” Nd is found in strange alkali-rich or undersaturated volcanics. We recognize, however, that these are not primitive compositions for Sr, Nd and Pb, because we have constraints on parent-daughter ratios, and understand their behavior during magmatism. Not so for the (U+Th)-He system. If He is more compatible than U, then high $^3\text{He}/^4\text{He}$ is a signature expected for melt-depletion, similar to the effect seen in MORBs for Sr and Pb. Thus, the parochial view of ^3He must be critically evaluated as we construct and define our models.